



HAL
open science

Electronic transport through domain walls in ferromagnetic nanowires: Co-existence of adiabatic and non-adiabatic spin dynamics

Victor A. Gopar, Dietmar Weinmann, Rodolfo A. Jalabert, Robert Stamps

► **To cite this version:**

Victor A. Gopar, Dietmar Weinmann, Rodolfo A. Jalabert, Robert Stamps. Electronic transport through domain walls in ferromagnetic nanowires: Co-existence of adiabatic and non-adiabatic spin dynamics. *Physical Review B: Condensed Matter and Materials Physics (1998-2015)*, 2004, 69, pp.14426. 10.1103/PhysRevB.69.014426 . hal-00000514

HAL Id: hal-00000514

<https://hal.science/hal-00000514>

Submitted on 22 Jul 2003

HAL is a multi-disciplinary open access archive for the deposit and dissemination of scientific research documents, whether they are published or not. The documents may come from teaching and research institutions in France or abroad, or from public or private research centers.

L'archive ouverte pluridisciplinaire **HAL**, est destinée au dépôt et à la diffusion de documents scientifiques de niveau recherche, publiés ou non, émanant des établissements d'enseignement et de recherche français ou étrangers, des laboratoires publics ou privés.

Electronic transport through domain walls in ferromagnetic nanowires: Co-existence of adiabatic and non-adiabatic spin dynamics

Victor A. Gopar,^{1,2} Dietmar Weinmann,¹ Rodolfo A. Jalabert,¹ and Robert L. Stamps³

¹*Institut de Physique et Chimie des Matériaux de Strasbourg,
UMR 7504 (CNRS-ULP), 23 rue du Loess, BP 43, 67034 Strasbourg Cedex 2, France*

²*Institut für Theorie der Kondensierten Materie,*

Universität Karlsruhe, Postfach 6980, 76128 Karlsruhe, Germany

³*Department of Physics, University of Western Australia, Nedlands WA 6907, Australia*

We study the effect of a domain wall on the electronic transport in ferromagnetic quantum wires. Due to the transverse confinement, conduction channels arise. In the presence of a domain wall, spin up and spin down electrons in these channels become coupled. For very short domain walls or at high longitudinal kinetic energy, this coupling is weak, leads to very few spin flips, and a perturbative treatment is possible. For very long domain wall structures, the spin follows adiabatically the local magnetization orientation, suppressing the effect of the domain wall on the total transmission, but reversing the spin of the electrons. In the intermediate regime, we numerically investigate the spin-dependent transport behavior for different shapes of the domain wall. We find that the knowledge of the precise shape of the domain wall is not crucial for determining the qualitative behavior. For parameters appropriate for experiments, electrons with low longitudinal energy are transmitted adiabatically while the electrons at high longitudinal energy are essentially unaffected by the domain wall. Taking this co-existence of different regimes into account is important for the understanding of recent experiments.

PACS numbers: 72.10.-d, 75.47.Jn, 73.23.-b, 75.75.+a

I. INTRODUCTION

A new kind of electronic devices taking advantage of the electron spin have been developed during the last years. The influence of the spin on electronic transport attracts considerable interest since early experiments in multi-layered magnetic structures have shown that the resistance is considerably increased in the case of an anti-parallel magnetization of the layers, as compared to a parallel configuration^{1,2}. This is at the base of the so-called Giant Magneto-Resistance (GMR), which is already used in the read-heads of commercial high performance hard-disks.

In magnetic configurations that are obtained when one substitutes the non-magnetic spacer layer between the ferromagnets by domain walls³, the effect of a magnetic domain wall on the electronic transport properties has become a subject of great interest. In particular, the effect of a *single domain wall* on the resistance of a ferromagnetic nanowire has been measured for electro-deposited cylindrical Co wires down to 35 nm in diameter⁴, and thin polycrystalline Co films having a thickness of 42 nm and a width down to 150 nm⁵. The results of both experiments indicate that, besides negative contributions from the anisotropic magneto-resistance, the domain wall scattering yields a positive contribution to the resistance.

The prospect of interesting technological applications of magneto-electronic devices exploiting the spin degree of freedom of the electrons together with its importance from the fundamental point of view has strongly motivated theoretical studies of spin-dependent electronic transport.

Many efforts have been made in order to explain the electronic transport, in particular the enhancement of the magneto-resistance in these spin-dependent electronic devices. For example, a Boltzmann equation has been applied to study the resistance of multi-layered magnetic/non-magnetic structures when the spin-diffusion length is larger than the mean free path⁶. While the electronic spin is expected to follow adiabatically a very slowly varying magnetization⁷, the deviations from this adiabatic behavior, which are due to the finite length of the domain wall, lead to a so-called mistracking of the spin, and result in a GMR-like enhancement of the magneto-resistance in multi-domain wall configurations³. Including spin-dependent scattering, the mistracking and the resulting magneto-resistance have been calculated for such a system, within the so-called two-band model⁸, which consists in a simplification of the complicated band structure of a ferromagnetic metal.

An outstanding problem in magnetism is a fully consistent description of transport and thermal properties in terms of electronic states calculated from first principles. Despite remarkable progress in the past twenty years, such a description does not yet exist in a form suitable for predicting features such as domain wall structures in non-equilibrium situations. As such, it is reasonable to search for suitably simplified model descriptions that capture the essence of the important physics involved. In the present case, a two-band model is useful for the study of how the geometrical characteristics of a magnetic domain wall affect electron transport. We make a distinction between spatially extended electronic states that contribute strongly to conduction and more localized states that contribute strongly to the formation of

local magnetic moments. For the transition metals, this model assumes that exchange correlations between electrons in primarily d -like orbitals are largely responsible for the formation of magnetic moments leading to the microscopic magnetization. The s -like orbitals contribute much less strongly to the magnetization and instead interact relatively weakly with the local moments via a contact interaction term. These types of s - d interaction models have proven very useful in the past for discussions of indirect exchange interactions in magnetic transition metal multilayers.

In our work we therefore assume that the domain wall represents a stable magnetic state with an energy above the ferromagnet ground state. The exact shape and dimensions of the wall are determined by exchange correlation energies and spin orbit interactions primarily affecting electrons associated with the magnetization of the wall. These interactions are small perturbations on the conduction electron states, and the interaction between conduction electrons and the domain wall is represented by a simple contact potential. In a single electron picture, the wall appears as a spatially varying spin dependent potential for the conduction electrons. The magnitude of the splitting between the spin up and spin down potentials is taken as a free parameter that is related to the exchange correlation energy of the electrons involved in forming the wall, and the contact potential describing interaction of conduction electrons with the effective potential associated with the wall structure. In the following we refer to this contact potential between conduction electrons and the magnetization as an 'exchange interaction' although it is quite distinct from the exchange interaction used to parameterize the interactions leading to magnetic ordering.

In thin ballistic quantum wires and narrow constrictions or point contacts, the lateral confinement of the electronic wave-functions leads to the emergence of quantized transport channels. As a consequence, the conductance is quantized and exhibits steps of e^2/h as a function of the Fermi energy^{9,10}. Nakanishi and Nakamura¹¹ considered the conductance of very narrow quantum wires including the effect of a domain wall. A perturbative approach allowed them to study the effect of a very short domain wall on the conductance steps. Imamura and collaborators¹² calculated the conductance of a point contact connecting two regions of a ferromagnet having parallel or anti-parallel magnetization directions. Within an $s - d$ two-band model, they numerically obtained a non-monotonic dependence of the domain wall contribution to the resistance on the width of the point contact.

There have been attempts to compare different approaches to the calculation of the domain wall magneto-resistance (DWMR), which point towards the importance of including more realistic band structures. In the ballistic case, van Hoof and collaborators¹³ calculated the DWMR for an adiabatic model where the magnetization direction changes very slowly along the wire, using an extension of the standard band structure calculation to

include an infinite spin spiral, as well as a "linear" model, where the magnetization turns in a finite region at a constant rate. These two approaches yield a much larger effect than a two-band model, where corrections with respect to an infinitely long domain wall are calculated. On the other hand, first principle calculations for the case of abrupt magnetization interfaces yield a DWMR which is orders of magnitude larger than for the other models that take into account realistic domain wall lengths.

It then seems necessary to develop more accurate treatments within the two-band model in order to understand the crossover from the abrupt domain wall situation to the adiabatic regime. Since we are working with nanowires, obvious transverse quantization effects appear, which are more easily tractable within a two-band model. Moreover, the two-band model allows to easily obtain the transmission coefficients with and without spin flip, making it possible to study the mistracking effect in finite length domain walls and its GMR-like consequences. Finally, given the typical experimental parameters, it would be important to go beyond the ballistic limit. Taking into account disorder within a two-band model seems much more doable than in the framework of a band structure calculation.

In this paper, we study the effect of a domain wall on the conductance of a nanowire within the two-band model, comparing different shapes and sizes of the domain wall. Focusing on the contribution of the spin-dependent scattering of the domain wall, we do not consider material-dependent contributions to the resistance like the anisotropic magneto-resistance.

After presenting our model in section II, we consider the perturbative regime of weak spin coupling induced by the domain wall in section III. From a comparison of different domain wall shapes, we shall extract the relevant parameters governing the transmission through the domain wall with and without spin-flip processes. While this applies to short domain walls, in section IV we study the transport in the general case of a strong spin coupling induced by the domain wall, which allows to treat domain walls of arbitrary length. We present the deviations from the full transmission with spin rotation following the local magnetic structure expected for infinitely long domain walls, which is due to finite domain wall length, and treat the most interesting crossover regime. This case is relevant since typical experiments^{4,5} are far from the thin wall regime, but not really in the adiabatic limit in which the length of the domain walls is large.

II. MODEL

We consider a wire along the z axis with a domain wall, and choose the origin ($z = 0$) in the middle of the wall (see Fig. 1). As explained above, we work within the two-band model, where the d electrons are responsible for the magnetization and the current is carried by the s electrons. Therefore, we write for the latter an effective

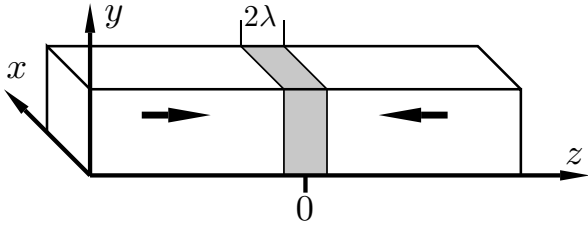


FIG. 1: Sketch of a ferromagnetic quantum wire containing a domain wall (grey region), for the example geometry of a square cross-section. The arrows indicate the magnetization directions far from the domain wall, for the case of a Néel wall.

Hamiltonian

$$H = -\frac{\hbar^2}{2m}\nabla^2 + \frac{\Delta}{2}\vec{f}(\vec{r}) \cdot \vec{\sigma}, \quad (1)$$

where Δ is the spin splitting of the s electrons due to the exchange coupling with the d electrons and $\vec{\sigma}$ is the vector of the Pauli matrices. The unit vector \vec{f} represents the direction of the local magnetization. Its functional dependence describes the shape of the domain wall. The lateral confinement present in a nanowire may have a considerable influence on this shape, leading to domain walls which are altered as compared to the case of bulk domain walls^{5,14,15,16,17}. In addition, a spin-polarized current through the domain wall creates a torque which can alter its shape¹⁸. Working in the linear response regime of low current, we do not need to take into account this back-action of the conduction electrons on the magnetic structure.

Assuming that the magnetization only depends on z , we will therefore be interested in comparing different functional forms of the kind $\vec{f} = \{f_x(z), 0, f_z(z)\}$. This choice does not imply a loss of generality and corresponds to a so-called “Néel wall”, where the magnetization is parallel to the wire axis in the leads far from the domain wall (arrows in Fig. 1), and turns inside the x - z plane parallel to this wire axis when going through the wall.

The assumption $\vec{f}(\vec{r}) = \vec{f}(z)$ allows us to separate the transverse and longitudinal parts of the Hamiltonian (1). The transverse quantization gives rise to transport channels with quantum numbers n_1 and n_2 , and an energy E_{n_1, n_2} . The density of channels $\rho = 2\pi mA/\hbar^2$ (where A is the cross-section of the transverse area of the wire) is equal to that of a two-dimensional system, and thus independent of the energy and the shape of the cross-section. For the example of a wire with a square cross-section of side w , we have

$$E_{n_x, n_y} = \frac{\hbar^2}{2m} \left(\left(\frac{\pi n_x}{w} \right)^2 + \left(\frac{\pi n_y}{w} \right)^2 \right). \quad (2)$$

Far away from the domain wall, the orbital parts of the eigenstates are products of transverse channels and

longitudinal plane waves. Since $\lim_{z \rightarrow \pm\infty} f_z(z) = \pm 1$, the associated eigenenergies for spin up are

$$E_{\uparrow} = E_{n_1, n_2} + \frac{\hbar^2 k_z^2}{2m} \pm \frac{\Delta}{2}, \quad (3)$$

while for spin down we have

$$E_{\downarrow} = E_{n_1, n_2} + \frac{\hbar^2 k_z^2}{2m} \mp \frac{\Delta}{2}. \quad (4)$$

The domain wall leads to the scattering of these states and the conductance (in units of e^2/h) is given by the Landauer formula

$$g = \sum_{n_1, n_2} \sum_{\sigma, \sigma'} T_{n_1, n_2}^{\sigma, \sigma'}(E_F), \quad (5)$$

where the sum is done over the occupied channels. $T_{n_1, n_2}^{\sigma, \sigma'}$ is the transmission coefficient in the channel (n_1, n_2) , for scattering of electrons with spin σ into spin σ' . Such a coefficient only depends on the longitudinal energy

$$\epsilon = E_F - E_{n_1, n_2} \quad (6)$$

as

$$T_{n_1, n_2}^{\sigma, \sigma'}(E_F) = T^{\sigma, \sigma'}(\epsilon). \quad (7)$$

Therefore, for each channel (n_1, n_2) , we are left with an effective one-dimensional problem at energy ϵ .

In order to determine the transmission probability $T^{\sigma, \sigma'}(\epsilon)$, we write the spinor wave-function in the up-down basis (with fixed, z -independent spin orientations) as

$$|\psi(z)\rangle = \phi_{\uparrow}(z)|z, \uparrow\rangle + \phi_{\downarrow}(z)|z, \downarrow\rangle, \quad (8)$$

where $|z, \uparrow\rangle$ has to be interpreted as the tensor product of the position eigenvector $|z\rangle$ and the spin up state $|\uparrow\rangle$. The Schrödinger equation with the Hamiltonian (1) leads to a system of coupled differential equations for the components $\phi_{\uparrow}(z)$ and $\phi_{\downarrow}(z)$:

$$\frac{d^2}{dz^2}\phi_{\uparrow} + \frac{2m}{\hbar^2} \left(\epsilon - \frac{\Delta}{2} f_z \right) \phi_{\uparrow} = \frac{2m}{\hbar^2} \frac{\Delta}{2} f_x \phi_{\downarrow} \quad (9a)$$

$$\frac{d^2}{dz^2}\phi_{\downarrow} + \frac{2m}{\hbar^2} \left(\epsilon + \frac{\Delta}{2} f_z \right) \phi_{\downarrow} = \frac{2m}{\hbar^2} \frac{\Delta}{2} f_x \phi_{\uparrow}. \quad (9b)$$

While the term containing f_z plays the role of a spin-dependent potential, the transverse component f_x of the wall profile is responsible for the coupling between the spinor components ϕ_{\uparrow} and ϕ_{\downarrow} . The scattering solutions of Eq. (9) are then needed to calculate the transmission coefficients, and therewith the conductance through the domain wall.

For the extreme case of an abrupt domain wall, when f_z has a jump from -1 to 1 , the right-hand-side of Eqs. (9) vanishes, and spin up and spin down electrons remain

uncoupled. The only effect of the discontinuity of f_z is a spin-dependent potential step of height $\pm\Delta$ for spin up/down electrons. Incoming spin up electrons having longitudinal energy $\epsilon < \Delta/2$ cannot overcome this step and are reflected with probability one. Since the density of conduction channels is independent of the energy for wires having a two-dimensional cross-section, this mechanism blocks a fraction $\Delta/2E_F$ of the conduction channels¹⁹, all of which exhibit perfect transmission in the absence of the domain wall. If one neglects the effect of the potential step on electrons having higher longitudinal energy ($\epsilon > \Delta/2$), this channel blocking mechanism leads to a relative change in conductance

$$\frac{\delta g}{g} = -\frac{\Delta}{2E_F}, \quad (10)$$

due to the presence of the domain wall. Taking into account the spin conserving reflections for $\epsilon > \Delta/2$ leads²⁰ (in the limit $E_F \gg \Delta$) to an increase of the effect by a factor 4/3.

The precise shape of the actual domain wall present in an experimental measurement (which is very difficult to know) would in principle be needed to determine the scattering states. In addition, it is not possible to find an analytical solution of Eqs. (9) for arbitrary domain walls. This is why we introduce various models of a domain wall, and approximate analytical, as well as numerical calculations.

In the bulk, when the magnetization always remains parallel to the domain wall, we have the so-called Bloch walls, whose shape was originally calculated by minimizing the total free energy in the thermodynamic limit²¹. In this case, $\vec{f}(\vec{r})$ is given by

$$\vec{f}(z) = \left\{ \tanh\left(\frac{z}{\lambda}\right), \operatorname{sech}\left(\frac{z}{\lambda}\right), 0 \right\}, \quad (11)$$

where λ is the length scale of the domain wall. The lateral confinement present in a nanowire will certainly alter the previous functional form of \vec{f} . Moreover, an easy magnetization axis in the direction of the nanowire will result in a Néel wall, modified by the transverse confinement. Such effects have been recently discussed in the literature^{15,16,17}.

The variety of possible domain wall structures motivates us to consider different domain wall profiles: linear, trigonometric and extended (defined below), in order to determine the influence of the domain wall shape on the conductance of the wire. As we will see below, while most of the effects are not very sensitive to the details of the wall, the signature of the particular domain wall appears in some regimes.

A possible starting point is to assume that the Néel-like confined domain wall has components with the same functional form as in Eq. (11). In this case we will consider the “extended” domain wall defined by the magnetization direction

$$\vec{f}^{\text{(ex)}}(z) = \left\{ \operatorname{sech}\left(\frac{z}{\lambda}\right), 0, \tanh\left(\frac{z}{\lambda}\right) \right\}. \quad (12)$$

As compared with the situation of a Bloch wall, this leads to a permutation of the spatial variables in Eqs. (9), and does not change the results for the transmission coefficients. This is why in the limit of high electron energy we can compare our results with the ones of Cabrera and Falicov²², who considered Bloch domain walls.

In the case of weak coupling between the spin up and down states described by Eq. (9) and short domain walls it is reasonable to approximate f_z in the wall profile with a linear function of position

$$\vec{f}^{\text{(lin)}}(z) = \begin{cases} \left\{ \sqrt{1 - (z/\lambda)^2}, 0, z/\lambda \right\}, & \text{for } |z| < \lambda \\ \left\{ 0, 0, \operatorname{sgn}(z) \right\}, & \text{for } |z| \geq \lambda. \end{cases} \quad (13)$$

The semi-circle form of the coupling term f_x in this “linear” wall ensures that $|\vec{f}(z)|^2 = 1$. This is an important difference as compared to our previous work¹⁹, where the conservation of the absolute value of the magnetization was not respected. The above constraint has only quantitative consequences in the short wall limit which play a role when comparing different wall profiles, but becomes crucial for longer domain walls in the adiabatic regime.

For an arbitrary domain wall, the extension of the standard recursive Green function method^{23,24} to take into account the spin degree of freedom (in a tight binding setup) allows us to calculate the transmission and reflection coefficients $T_{\uparrow\uparrow}$, $T_{\uparrow\downarrow}$, $R_{\uparrow\uparrow}$ and $R_{\uparrow\downarrow}$.

The case of a “trigonometric” domain wall

$$\vec{f}^{\text{(tri)}}(z) = \begin{cases} \left\{ \cos\frac{\pi z}{2\lambda}, 0, \sin\frac{\pi z}{2\lambda} \right\}, & \text{for } |z| < \lambda \\ \left\{ 0, 0, \operatorname{sgn}(z) \right\}, & \text{for } |z| \geq \lambda \end{cases} \quad (14)$$

admits an exact solution for the wave-function inside the domain wall²⁵ which has recently been used to calculate the torque that is due to a spin-polarized current¹⁸. We use the exact solution to determine the scattering properties of the domain wall. Details are presented in Appendix A.

By comparing with this exact analytic solution we checked the accuracy of the numerical method, as well as the absence of lattice effects for the parameters that we work with.

III. WEAK COUPLING

The problem can be treated at the analytical level when the differential equations (9) are only weakly coupled. This is the case when the domain wall (in which the spin-flip terms f_x are non-zero) is very short, or when the longitudinal energy of the electron is very high such that the transmitted electrons spend only a short time inside the domain wall region.

Then, we treat the system of coupled differential equations (9) iteratively, considering the spin-flip terms on the right-hand-side as a perturbation. Within this approach, the solution to the homogeneous differential equation (9a) (in which the spin-flip terms induced by f_x are set to

zero) is injected in the spin-flip term of the second differential equation (9b). This method was used in Ref. [19], where a mechanism of channel blocking by a domain wall was proposed as a source of resistance in short ferromagnetic quantum wires. The starting point of this approach, which we present here for the example of a linear domain wall as described by (13), is an incoming majority (spin-up) electron from the left ϕ_{\uparrow}^H , and $\phi_{\downarrow}^H = 0$. Outside the domain wall region, ϕ_{\uparrow}^H reads

$$\phi_{\uparrow}^H(z) = e^{ikz} + r_{\uparrow\uparrow}e^{-ikz} \quad \text{for } z < -\lambda \quad (15a)$$

$$\phi_{\uparrow}^H(z) = t_{\uparrow\uparrow}e^{ik'z} \quad \text{for } z > \lambda, \quad (15b)$$

with the wave-numbers

$$k = \sqrt{\frac{2m}{\hbar^2} \left(\epsilon + \frac{\Delta}{2} \right)} \quad (16a)$$

$$k' = \sqrt{\frac{2m}{\hbar^2} \left(\epsilon - \frac{\Delta}{2} \right)}. \quad (16b)$$

For $-\lambda < z < \lambda$, the homogeneous solution of Eq. (9a) is

$$\begin{aligned} \phi_{\uparrow}^H(z) = & \alpha \text{Ai} \left[p^{2/3} \left(-\frac{2\epsilon}{\Delta} + \frac{z}{\lambda} \right) \right] \\ & + \beta \text{Bi} \left[p^{2/3} \left(-\frac{2\epsilon}{\Delta} + \frac{z}{\lambda} \right) \right] \end{aligned} \quad (17)$$

with the usual Airy functions Ai and Bi, and the dimensionless parameter p defined by

$$p = \left(\frac{m}{\hbar^2} \Delta \right)^{1/2} \lambda = \left(\frac{\Delta}{2E_F} \right)^{1/2} k_F \lambda. \quad (18)$$

The coefficients α and β , as well as $t_{\uparrow\uparrow}$ and $r_{\uparrow\uparrow}$, are obtained from the matching of the expressions (15) and (17) at $z = \pm\lambda$. For $\epsilon < \Delta/2$, we have imaginary k' . The transmission without spin-flip is zero and $|r_{\uparrow\uparrow}| = 1$. For $\epsilon > \Delta/2$, the transmission without spin-flip is finite.

The first-order correction from the spin-conserving scattering is then obtained by injecting ϕ_{\uparrow}^H as the inhomogeneous term in the differential equation (9b) for ϕ_{\downarrow} . Since we do not have incoming spin-down electrons, outside the domain wall region we take the outgoing plane waves

$$\phi_{\downarrow}^{(1)}(z) = r_{\uparrow\downarrow}e^{-ik'z} \quad \text{for } z < -\lambda \quad (19a)$$

$$\phi_{\downarrow}^{(1)}(z) = t_{\uparrow\downarrow}e^{ikz} \quad \text{for } z > \lambda. \quad (19b)$$

For $-\lambda < z < \lambda$ the general solution can be written as a linear combination of Airy functions plus a particular solution $\phi^P(z)$

$$\begin{aligned} \phi_{\downarrow}^{(1)}(z) = & \alpha_1 \text{Ai} \left[-p^{2/3} \left(\frac{2\epsilon}{\Delta} + \frac{z}{\lambda} \right) \right] \\ & + \beta_1 \text{Bi} \left[-p^{2/3} \left(\frac{2\epsilon}{\Delta} + \frac{z}{\lambda} \right) \right] + \phi^P(z). \end{aligned} \quad (20)$$

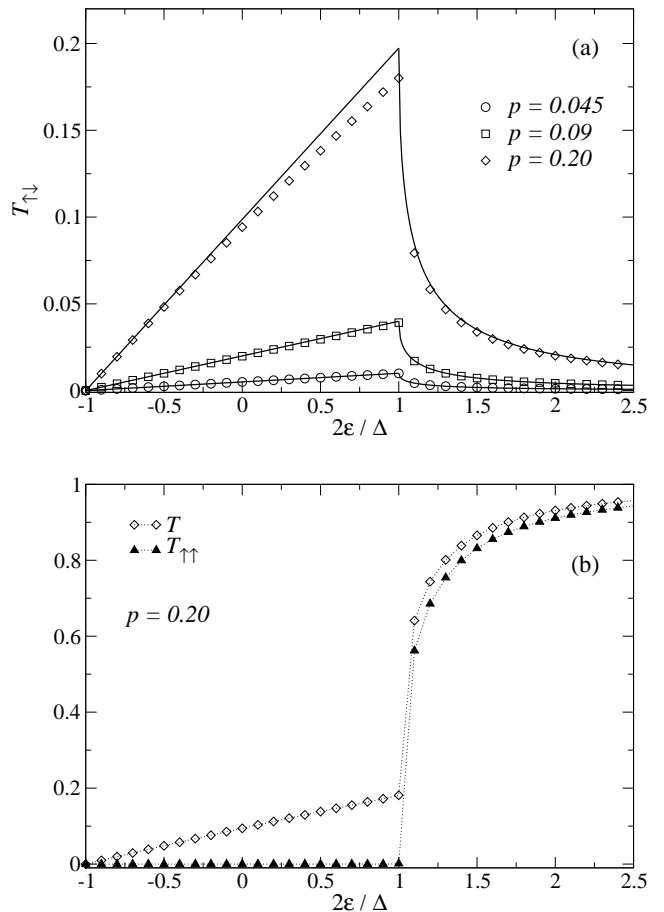


FIG. 2: (a) Perturbative results for $T_{\uparrow\downarrow}$ from Eqs. (22) and (23) (solid lines) for three values of p , compared with the corresponding full numerical results (circles, squares and diamonds) for the linear domain wall. (b) The total transmission T and $T_{\uparrow\uparrow}$ (diamonds and triangles, respectively) for $p = 0.20$.

Spin-flip processes are now included in the description, and electrons undergoing a spin-flip can be transmitted even for energies $\epsilon < \Delta/2$. The parameters α_1 and β_1 and the coefficients $t_{\uparrow\downarrow}$ and $r_{\uparrow\downarrow}$ are determined from the matching of (19) and (20).

A. Long wavelength limit

In the limit of a short wall, when the wavelength of the incoming electron is much longer than the domain wall, the linear approximation of the Airy functions allows us to write for $\epsilon > \Delta/2$

$$T_{\uparrow\uparrow} = |t_{\uparrow\uparrow}|^2 = \frac{4kk'}{(k+k')^2 + 4(\lambda kk')^2} \quad (21a)$$

$$R_{\uparrow\uparrow} = |r_{\uparrow\uparrow}|^2 = \frac{(k-k')^2 + 4(\lambda kk')^2}{(k+k')^2 + 4(\lambda kk')^2}. \quad (21b)$$

Obviously, for $\lambda \rightarrow 0$ we recover the well-known results for a step potential²⁶.

For $\epsilon < \Delta/2$, the transmission probability with spin-flip is given by

$$T_{\uparrow\downarrow} = |t_{\uparrow\downarrow}|^2 = C^2 p^2 \left(1 + \frac{2\epsilon}{\Delta}\right). \quad (22)$$

For $\epsilon > \Delta/2$,

$$T_{\uparrow\downarrow} = 4C^2 p^4 \frac{4(x^2 - 1) + p^2(x + 1)(\frac{2}{3}(x - 1) - 1/p^2)^2}{((\sqrt{x+1} + \sqrt{x-1})^2 + 4p^2(x^2 - 1))^2} \quad (23)$$

is obtained, with $x = 2\epsilon/\Delta$ and the prefactor C defined by

$$C = \frac{1}{\lambda} \int_{-\infty}^{\infty} dz f_x(z). \quad (24)$$

In Fig. 2 (a) we show $T_{\uparrow\downarrow}$ from Eqs. (22) and (23) as a function of $2\epsilon/\Delta$, together with numerical calculations for three different values of p . We can see an excellent agreement for the smallest values of p . When the value of p is increased, deviations appear first at energies close to $\Delta/2$. These features are consistent with the fact that the linear approximation of the Airy functions is justified in the small p limit, and becomes increasingly better for small energies.

The total transmission $T = T_{\uparrow\downarrow} + T_{\uparrow\uparrow}$ (Fig. 2 (b)) is dominated by the large transmission without spin-flip for $\epsilon > \Delta/2$. This feature justifies the ‘‘channel blocking’’ picture proposed for short domain walls in Ref. [19], where the presence of the wall suppresses almost completely the transmission at energies $\epsilon < \Delta/2$ ($T_{\uparrow\downarrow}$ is only a small correction for $\epsilon < \Delta/2$ and negligible for $\epsilon \gg \Delta/2$). Neglecting what happens for $\epsilon > \Delta/2$, we have $\delta g/g = (-1 + (Cp)^2)\Delta/2E_F$.

In the limit of short domain walls, we have found that the dependence of the transmission coefficients on the shape of the wall is only through the integral over f_x which enters in the prefactor C . For the linear, trigonometric and extended domain walls, C takes the values $\pi/2$, $4/\pi$ and π , respectively. Such a scaling is shown in Fig. 3, where the transmissions $T_{\uparrow\downarrow}$ divided by the coupling strength $(Cp)^2$ for the different domain wall shapes coincide for all energies, except those close to $\Delta/2$.

B. Short wavelength limit

The perturbative approach is not only applicable for short walls and low energies (as in section III A), but for general domain wall parameters as well, provided that $\epsilon \gg (\Delta\lambda/\hbar)^2/m$. That is, when the time that the electron spends inside the domain wall is much shorter than the spin precession period, and therefore the spin-flips are very unlikely. In this limit, the WKB approximation of the scattering wave-functions for the linear domain wall

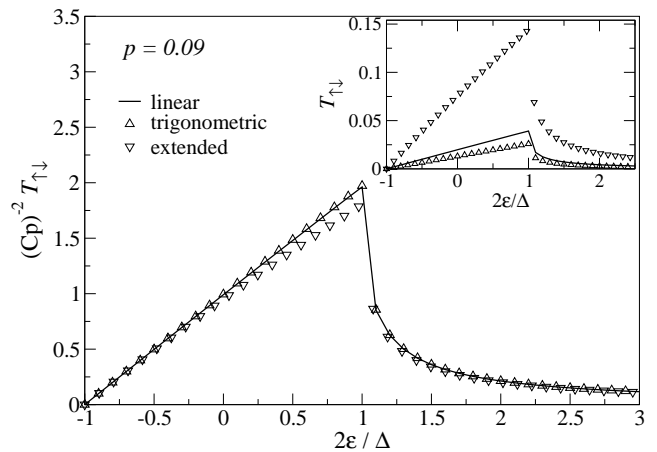


FIG. 3: The transmission $T_{\uparrow\downarrow}$ divided by the coupling strength $(Cp)^2$ for the linear, trigonometric and extended domain walls (solid line, up and down triangles, respectively). The inset shows the results for $T_{\uparrow\downarrow}$ for the same value of $p = 0.09$, before dividing by the corresponding value of $(Cp)^2$.

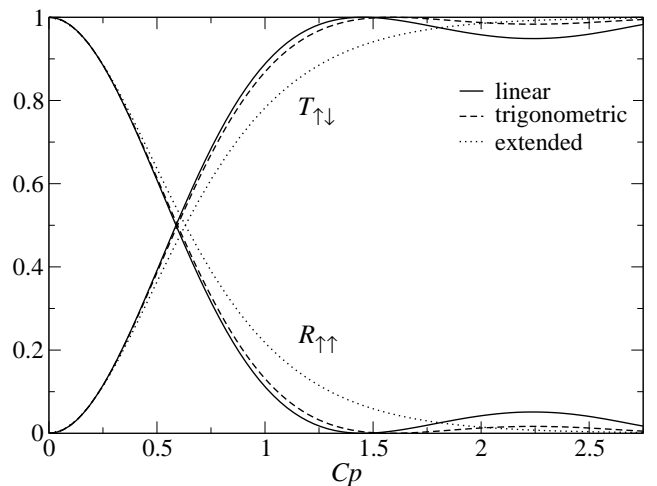


FIG. 4: The coefficients $T_{\uparrow\downarrow}$ and $R_{\uparrow\uparrow}$ as a function of Cp for the three different domain wall shapes, at $\epsilon = 0.95\Delta/2$. An oscillatory behavior for the linear and trigonometric walls is found as a consequence of the edges at the connection to the leads.

model (Eq. (13)) yields the reflection and transmission

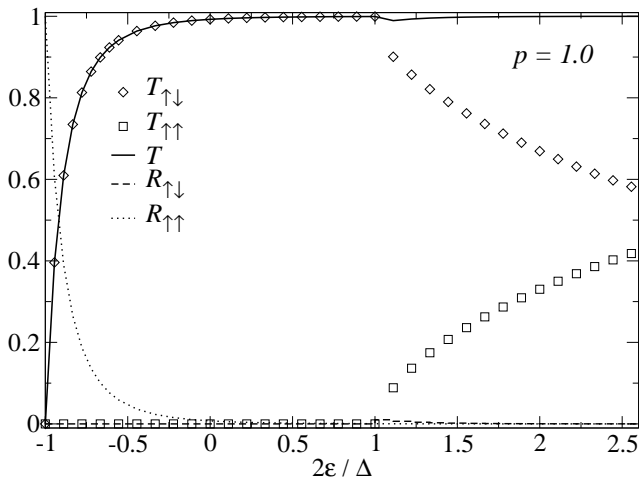


FIG. 5: Transmission and reflection coefficients in the intermediate regime ($p = 1$) for the extended domain wall geometry (12). A large transmission with spin-flip (diamonds) is found for energies $\epsilon < \Delta/2$ in this regime, where the transport is adiabatic.

coefficients

$$R_{\uparrow\uparrow} = \left(\frac{\Delta}{4\epsilon}\right)^2 \frac{\sin^2(2k\lambda)}{(2k\lambda)^2} \quad (25)$$

$$R_{\uparrow\downarrow} = \left(\frac{C\Delta}{8\epsilon}\right)^2 \sin^2(2k\lambda) \quad (26)$$

$$T_{\uparrow\downarrow} = \left(\frac{C\Delta}{8\epsilon}\right)^2 (2k\lambda)^2 \quad (27)$$

$$T_{\uparrow\uparrow} = 1 - R_{\uparrow\uparrow} - R_{\uparrow\downarrow} - T_{\uparrow\downarrow}. \quad (28)$$

Thus, for energies $\epsilon \gg \Delta$ all scattering coefficients, except the transmission without spin-flip, are very small. Therefore, in first approximation we can neglect the effect of the domain wall for electrons with high longitudinal energies. The conductance associated with the domain wall is then determined by the low-energy electrons¹⁹. The algebraic decay in Δ/ϵ is less pronounced than the exponential suppression obtained by Cabrera and Falicov²². Such a difference arises from the sharp edges at $z = \pm\lambda$ in the linear domain wall model we used for this calculation.

IV. STRONG COUPLING

If we are interested in energies $\epsilon \simeq \Delta/2$ and not necessarily short walls, the previous picture has to be modified. The linear approximation and the perturbative treatment (involving only one spin-flip) in the wall region are no longer justified. Beyond the perturbative regime, the detailed shape of the domain wall might become relevant.

In Fig. 4, we present $T_{\uparrow\downarrow}$ and $R_{\uparrow\uparrow}$ as a function of the coupling strength for different domain wall shapes and

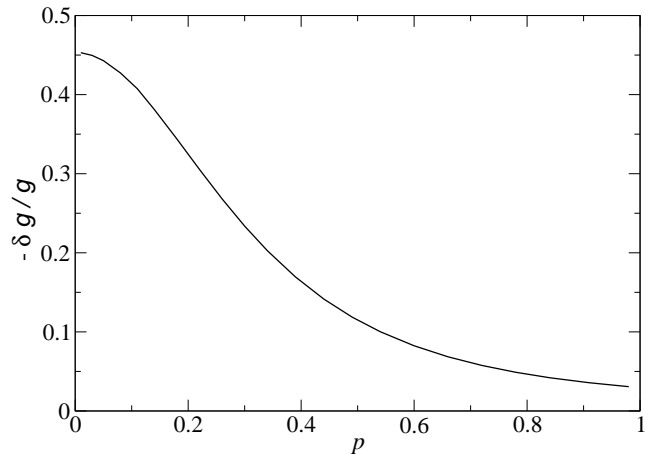


FIG. 6: The relative change in conductance $\delta g/g$ caused by the presence of a domain wall (extended shape), for $E_F = 2\Delta$.

an energy of the order of $\Delta/2$. As discussed in the previous section, it is for these energies that a dependence on the detailed shape of the domain wall appears first when departing from the weak coupling limit ($Cp \ll 1$). We can see from Fig. 4 that the transmissions (reflections) for the different domain wall shapes coincide for small values of Cp . Even for stronger couplings, the different models do not show very important differences in their behaviors. The only apparent difference are oscillations of the transmission coefficients as a function of p , which occur at intermediate p for linear and trigonometric domain walls. The origin of these oscillations is due to the edges of the domain wall region leading to Fabry-Perot like interferences. For a smooth domain wall structure such as the extended domain wall, the oscillations are absent. On the other hand, and as expected, $T_{\uparrow\downarrow} \rightarrow 1$ for all shapes in the limit of large p .

It is the limit of infinite domain wall length where the spin follows adiabatically the orientation of the local magnetization⁷, corresponding to a rotation from spin up to spin down in the external basis of fixed spin orientations. Electrons are transmitted with probability one through the wall, therefore $T_{\uparrow\downarrow} = 1$ and $T_{\uparrow\uparrow} = R_{\uparrow\uparrow} = R_{\uparrow\downarrow} = 0$. In this limit the detailed shape of a domain wall, having slow spatial spin rotation, is irrelevant. The adjustment of the spin to the direction of the local magnetization requires an infinite number of spin-flips (in the fixed basis), and obviously cannot be described by taking into account a small number of spin-flips as in the perturbative approach used for short domain walls. The condition for the local adjustment is that the Larmor precession of the spin around the local magnetization is much faster than the rotation of the local magnetization viewed by the traveling electron⁷. This condition of adiabaticity translates into $\Delta \gg (h/\lambda)\sqrt{\epsilon/m}$.

We then see that the adiabatic condition strongly depends on the longitudinal kinetic energy of the electrons.

In a quantum wire, at a finite value of λ , electrons with low longitudinal velocity are essentially adiabatic, while the channels with low transverse quantum numbers can be highly non-adiabatic. In calculating the conductance of a ferromagnetic quantum wire, we have to take into account the co-existence of adiabatic (low longitudinal energy) and non-adiabatic (high longitudinal energy) electrons. It then seems important to work out the crossover between the short wall and adiabatic limits, for different shapes of the domain wall.

For an intermediate value of p in the case of an extended domain wall, Fig. 5 shows that the behavior for $\epsilon < \Delta/2$ is radically different from the weak coupling case of section III. The weak coupling result of Eq. (22) is only valid at extremely low energies, and the $T_{\uparrow\downarrow}$ approaches one (adiabatic behavior) for longitudinal energies considerably lower than the step height. Above $\Delta/2$, $T_{\uparrow\downarrow}$ decreases monotonously with energy, returning to the weak coupling regime in the limit of large ϵ . At the same time, $T_{\uparrow\uparrow}$ increases towards one and T remains very close to perfect transmission for all energies.

Thus, almost all of the electrons with energy $\epsilon > \Delta/2$ are transmitted. However, while the spin of the transmitted electrons is changed by the domain wall for low ϵ and high p , the spin of electrons having high ϵ in domain walls of low p remains unaffected by the wall (see also Fig. 2 (a)). Therefore, in calculating the effect of the domain wall on the quantum conductance the modes with longitudinal energies in the interval $(-\Delta/2, \Delta/2)$ are most relevant¹⁹.

The conductance for the ideal ballistic case given in Eq. (5) is obtained by summing over all conductance channels. Fig. 6 shows an example of the resulting behavior for the difference in conductance between the cases without and with domain wall (normalized to the conductance without domain wall), as a function of the domain wall parameter p . We can see that the channel blocking effect due to the presence of the domain wall is rapidly suppressed upon increase of the coupling. Similar results have recently been obtained using a different numerical approach²⁰.

V. SUMMARY AND CONCLUSIONS

The effect of a single domain wall on the electronic transport in a ferromagnetic nanowire has been studied systematically in various parameter regimes. The domain wall leads to a coupling of spin up and spin down electrons in the conduction channels, which is proportional to the exchange energy of the conduction electrons and the length of the wall.

For an abrupt domain wall the step in the effective potential felt by the conduction electrons blocks the transmission of channels with low longitudinal energy. In the weak coupling limit, a perturbative approach is possible, leading to the lowest order correction to perfect channel blocking. In this case, the detailed shape of the do-

main wall is not relevant, and the transmission coefficients scale with the coupling strength. For a very long domain wall the spin of the electrons follows adiabatically the local effective magnetization and the conductance is unaffected by the domain wall, independently of its shape.

The intermediate coupling regime is most relevant for the domain walls that can be investigated experimentally. We have shown that the degree of adiabaticity of electrons at the Fermi energy strongly depends on their longitudinal kinetic energy. While the spin of electrons with low longitudinal energy essentially behaves adiabatically, the spin of electrons with high longitudinal energy is practically unaffected by the domain wall. The crossover between these two behaviors, as a function of the longitudinal energy of the electrons, has to be taken into account in calculating the conductance of the quantum wire.

Our analysis has been based on coherent scattering at the domain wall, which is connected to perfect leads. However, in realistic situations, the domain wall is not connected to scattering-free regions. The imperfections and impurities at both sides of the wall give rise to elastic scattering, which may be different for the two spin directions of the electrons. Though these coherent effects can in principle be taken into account in a scattering approach, such a coherent picture is not sufficient for wires which are longer than the phase coherence length. Since this is the case in typical experiments, we need in addition to take into account inelastic processes (like electron-phonon or spin-magnon scattering). The length of the leads over which the spin of the electrons is conserved can then be described phenomenologically by classical spin-dependent resistors²⁷. In this situation, the important part of the electrons which do not undergo spin-flip processes leads to an increase of the resistance due to the GMR mechanism. This picture is likely to be representative of the experimental situations [4,5]. More experimental and theoretical work concerning the various relaxation rates will be necessary to establish a complete quantitative understanding of the phenomenon.

Acknowledgments

We thank P. Falloon, H. Pastawski and X. Waintal for very useful discussions. In addition, we are grateful to H. Pastawski for crucial help in the implementation of the numerical method, and to X. Waintal for drawing our attention to the exact solution for the spin spiral of Ref. 25. This work received financial support from the European Union within the RTN program (Contract No. HPRN-CT-2000-00144). V.G. thanks the French Ministère délégué à la recherche et aux nouvelles technologies and the Center for Functional Nanostructures of the Deutsche Forschungsgemeinschaft (project B2.10) for support.

APPENDIX A: EXACT SOLUTION FOR THE TRIGONOMETRIC DOMAIN WALL

A particularly instructive case is that of a trigonometric domain wall (Eq. (14)) since an exact solution for the wave function inside the domain wall region can be obtained²⁵. Here we extend this approach to a scattering situation by matching the inner solutions with plane waves, which allows us to calculate the transmission and reflection amplitudes.

In addition to the external spin basis $\{|z, \uparrow\rangle, |z, \downarrow\rangle\}$, it is useful to introduce a local spin basis $\{|z, \uparrow^L\rangle, |z, \downarrow^L\rangle\}$, which corresponds to spin orientations parallel and antiparallel to the (rotating) local magnetization direction $\vec{f}(z)$, leading to

$$\begin{pmatrix} |z, \uparrow^L\rangle \\ |z, \downarrow^L\rangle \end{pmatrix} = R(z) \begin{pmatrix} |z, \uparrow\rangle \\ |z, \downarrow\rangle \end{pmatrix} \quad (\text{A1})$$

where the spin rotation matrix is given by

$$R(z) = \begin{pmatrix} \cos(az + \pi/4) & \sin(az + \pi/4) \\ -\sin(az + \pi/4) & \cos(az + \pi/4) \end{pmatrix} \quad (\text{A2})$$

with $a = \pi/4\lambda$. For $z = -\lambda$, R is simply the identity matrix (the local rotating basis coincides with the fixed one), and putting $z = \lambda$ corresponds to exchanging the spin directions between the local and fixed bases.

Inserting the spinor

$$|\psi(z)\rangle = \phi_{\uparrow}^L(z)|z, \uparrow^L\rangle + \phi_{\downarrow}^L(z)|z, \downarrow^L\rangle \quad (\text{A3})$$

into the Schrödinger equation corresponding to the Hamiltonian (1), we obtain

$$\left[\frac{d^2}{dz^2} - a^2 \right] \phi_{\uparrow}^L + \frac{2m}{\hbar^2} \left(\epsilon - \frac{\Delta}{2} \right) \phi_{\uparrow}^L = 2a \frac{d}{dz} \phi_{\downarrow}^L \quad (\text{A4a})$$

$$\left[\frac{d^2}{dz^2} - a^2 \right] \phi_{\downarrow}^L + \frac{2m}{\hbar^2} \left(\epsilon + \frac{\Delta}{2} \right) \phi_{\downarrow}^L = -2a \frac{d}{dz} \phi_{\uparrow}^L \quad (\text{A4b})$$

which is, in fact, Eq. (9) expressed in the local spin basis, for the case of a trigonometric domain wall. This system of coupled differential equations can be reduced to a 2×2 eigenvalue problem with the ansatz

$$\begin{pmatrix} \phi_{\uparrow}^L(z) \\ \phi_{\downarrow}^L(z) \end{pmatrix} = \exp(i\tilde{k}z) \begin{pmatrix} C_{\uparrow} \\ C_{\downarrow} \end{pmatrix}, \quad (\text{A5})$$

such that the solutions $(C_{\uparrow}, C_{\downarrow})$ and $2m\epsilon/\hbar^2$ are the eigenvectors and eigenvalues, respectively, of the matrix

$$M = \begin{pmatrix} \tilde{k}^2 + a^2 + m\Delta/\hbar^2 & 2i\tilde{k}a \\ -2i\tilde{k}a & \tilde{k}^2 + a^2 - m\Delta/\hbar^2 \end{pmatrix}. \quad (\text{A6})$$

The secular equation of M leads to the dispersion relations

$$\epsilon_{1,2} = \frac{\hbar^2}{2m} \left(\tilde{k}^2 + a^2 \pm \sqrt{4a^2\tilde{k}^2 + \frac{2m}{\hbar^2} \left(\frac{\Delta}{2} \right)^2} \right) \quad (\text{A7})$$

that is, the eigenenergies of the infinite spin spiral²⁵. For a closed spiral, the periodic boundary conditions would lead⁷ to quantized values of \tilde{k} . However, we are interested in a scattering problem, where the region in which the magnetization turns is connected to homogeneous ferromagnetic leads. We therefore express the general solution $(\phi_{\uparrow}^L, \phi_{\downarrow}^L)$ for a given energy as a linear combination of the four corresponding eigenstates of the spiral, and use the matching conditions between the domain wall region and the perfect leads at $z = \pm\lambda$. Taking into account the rotation of the local basis, and using the expressions given in Eqs. (15) and (19) for the wave-function outside the wall region, we get

$$\begin{aligned} e^{-ik\lambda} + r_{\uparrow\uparrow} e^{ik\lambda} &= \phi_{\uparrow}^L(-\lambda) \\ t_{\uparrow\uparrow} e^{ik'\lambda} &= -\phi_{\downarrow}^L(\lambda) \\ r_{\uparrow\downarrow} e^{ik'\lambda} &= \phi_{\downarrow}^L(-\lambda) \\ t_{\uparrow\downarrow} e^{ik\lambda} &= \phi_{\uparrow}^L(\lambda) \\ ik(e^{-ik\lambda} - r_{\uparrow\uparrow} e^{ik\lambda}) &= \frac{d}{dz} \phi_{\uparrow}^L(-\lambda) - a\phi_{\downarrow}^L(-\lambda) \\ ik't_{\uparrow\uparrow} e^{ik'\lambda} &= -\frac{d}{dz} \phi_{\downarrow}^L(\lambda) - a\phi_{\uparrow}^L(\lambda) \\ -ik'r_{\uparrow\downarrow} e^{ik'\lambda} &= \frac{d}{dz} \phi_{\downarrow}^L(-\lambda) + a\phi_{\uparrow}^L(-\lambda) \\ ikt_{\uparrow\downarrow} e^{ik\lambda} &= \frac{d}{dz} \phi_{\uparrow}^L(\lambda) - a\phi_{\downarrow}^L(\lambda). \end{aligned}$$

These conditions allow us to extract the amplitudes $t_{\uparrow\uparrow}$, $r_{\uparrow\uparrow}$, $t_{\uparrow\downarrow}$ and $r_{\uparrow\downarrow}$, as well as the precise form of the wave-function inside the domain wall. The resulting transmission coefficients are presented and discussed in Sec. IV.

¹ M.N. Baibich, J.M. Broto, A. Fert, F. Nguyen Van Dau, F. Petroff, P. Eitenne, G. Creuzet, A. Friederich, J. Chazelas, Phys. Rev. Lett. **61**, 2472 (1988).

² G. Binasch, P. Grünberg, F. Saurenbach, W. Zinn, Phys. Rev. B **39**, 4828 (1989).

³ J.F. Gregg, W. Allen, K. Ounadjela, M. Viret, M. Hehn, S.M. Thompson, J.M.D. Coey, Phys. Rev. Lett. **77**, 1580

(1996); M. Viret, D. Vignoles, D. Cole, J.M.D. Coey, W. Allen, D.S. Daniel, J.F. Gregg, Phys. Rev. B **53**, 8464 (1996).

⁴ U. Ebels, A. Radulescu, Y. Henry, L. Piraux, K. Ounadjela, Phys. Rev. Lett. **84**, 983 (2000).

⁵ G. Dumpich, T.P. Krome, B. Hausmanns, J. Magn. Magn. Mater. **248**, 241 (2002).

- ⁶ T. Valet, A. Fert, Phys. Rev. B **48**, 7099 (1993).
- ⁷ A. Stern, Phys. Rev. Lett. **68**, 1022 (1992).
- ⁸ P.M. Levy, S. Zhang, Phys. Rev. Lett. **79**, 5110 (1997).
- ⁹ B.J. van Wees, H. van Houten, C.W.J. Beenakker, J.G. Williamson, L.P. Kouwenhoven, D. van der Marel, C.T. Foxon, Phys. Rev. Lett. **60**, 848 (1988).
- ¹⁰ D.A. Wharam, T.J. Thornton, R. Newbury, M. Pepper, H. Ahmed, J.E.F. Frost, D.G. Hasko, D.C. Peacock, D.A. Ritchie, G.A.C. Jones, J. Phys. C: Solid State Phys. **21**, L209 (1988).
- ¹¹ K. Nakanishi, Y.O. Nakamura, Phys. Rev. B **61**, 11278 (2000).
- ¹² H. Imamura, N. Kobayashi, S. Takahashi, S. Maekawa, Phys. Rev. Lett. **84**, 1003 (2000).
- ¹³ J.B.A.N. van Hoof, K.M. Schep, A. Brataas, G.E.W. Bauer, P.J. Kelly, Phys. Rev. B **59**, 138 (1999).
- ¹⁴ P. Bruno, Phys. Rev. Lett. **83**, 2425 (1999).
- ¹⁵ I.L. Prejbeanu, L.D. Buda, U. Ebels, K. Ounadjela, Appl. Phys. Lett. **77**, 3066 (2000).
- ¹⁶ I.L. Prejbeanu, M. Viret, L.D. Buda, U. Ebels, K. Ounadjela, J. Magn. Magn. Mater. **240**, 27 (2002).
- ¹⁷ B. Hausmanns, T.P. Krome, G. Dumpich, E.F. Wassermann, D. Hinzke, U. Nowak, K.D. Usadel, J. Magn. Magn. Mater. **240**, 297 (2002).
- ¹⁸ X. Waintal, M. Viret, arXiv:cond-mat/0301293.
- ¹⁹ D. Weinmann, R.L. Stamps, R.A. Jalabert in *Electronic correlations: from meso- to nano-physics*, ed. by T. Martin, G. Montambaux, J. Trân Thanh Vân (EDP Sciences 2001).
- ²⁰ P.E. Falloon, R.L. Stamps, unpublished.
- ²¹ L.D. Landau, E.M. Lifshitz, *Course of Theoretical Physics*, Vol. 8, 1 Ed. Pergamon Press (1960).
- ²² G.G. Cabrera, L.M. Falicov, Phys. Stat. Sol. (b), **61**, 539 (1974); *ibid* **62**, 217 (1974).
- ²³ P.A. Lee, D.S. Fisher, Phys. Rev. Lett. **47**, 882 (1981).
- ²⁴ H.M. Pastawski, E. Medina, Rev. Mex. Fis. **47** S1, 1 (2001), and references therein, also available as arXiv:cond-mat/0103219.
- ²⁵ A. Brataas, G. Tatara, G.E.W. Bauer, Phys. Rev. B **60**, 3406 (1999).
- ²⁶ E. Merzbacher, *Quantum Mechanics*, John Wiley & Sons, 2 Ed. (1970).
- ²⁷ Y. Imry, *Introduction to Mesoscopic Physics*, Oxford University Press (New York 1997).